

Monolithic Systems Using Standard Three-Leg Inverter Supplying Independently Two Motors

Euzeli C. dos Santos Jr.
Federal Center of Technological
Education of Paraíba - CEFET PB
Cajazeiras, Paraíba, Brazil
Email: euzeli@dee.ufcg.edu.br

Cursino B. Jacobina
and Edison R. C. da Silva
Federal University of
Campina Grande - UFCG
Campina Grande, Paraíba, Brazil
Email: jacobina@dee.ufcg.edu.br

Hamid A. Toliyat
Electric Machines & Power
Electronics (EMPE) Laboratory
Texas A&M University - TAMU
College Station, Texas, USA
Email: toliyat@ee.tamu.edu

Abstract—This paper presents two series-connected motor drive system topologies. These configurations have been designed for applications in which it is necessary to control two motors independently by using a standard three-leg inverter. The systems will be called in this work as a monolithic systems, since both machines and the three legs inverter have been considered as the same product. The monolithic systems are seen as a potentially viable industrial solution for applications requiring one high-power (three-phase machine) and one low-power machine (single-phase machine). Furthermore, the paper presents: i) relevant characteristics of the systems, ii) pulse-width modulation techniques; iii) control strategies; iv) voltage and current analysis; v) unconventional induction machine design to improve the performance of the monolithic system; and vi) simulated and experimental results.

I. INTRODUCTION

In recent years a tendency of integrating the motor and its frequency converter into a single unit could be observed in a large number of papers [1], [2], [3]. The integration is done to reduce electromagnetic emissions, reduce installation size and commissioning costs, etc.

Another alternative for reducing the installation costs is the use of converter topologies with a minimized number of components. Then, the study of this kind of topologies is an important topic in power electronics since it may provide alternative solutions to reduce the cost of energy conversion process while preserving power quality [4], [5], [6].

In some cases, the components reduction is obtained by connecting in parallel two elements, chosen among grid, loads or machines [7]. In other cases, it is obtained by connecting grid and machines in series [8], or machines in series [9].

On the other hand, the standard three-leg converter represents the most common commercial inverter manufactured, since it is conceived for feeding a three-phase machine in a standard ac motor drive system. Therefore, there exist some applications that employ commercial three-leg inverters with two functions. For example, fed a three-phase machine and obtain a power factor correction [4], [10].

The paper presents two series-connected motor drive system topologies designed for applications in which it is necessary to control two motors independently by using a standard three-leg inverter. These systems will be called in this work

as a monolithic systems. The monolithic systems are seen as a potentially viable industrial solution for applications requiring one high-power (three-phase machine) and one low-power machine (single-phase machine). An example where such configurations can be useful is for feeding traction and compression machines in automotive applications [1]. Two proposed solutions employs standard three-leg converters and thus have less power devices than the direct solution in which the number of the switches is proportional to number of the machines. The configurations that will be examined are shown in Fig. 1.

Additionally, the paper presents: i) relevant characteristics of the converters, ii) pulse-width modulation techniques; iii) control strategies; iv) voltage and current analysis; v) unconventional induction machine design to improve the performance of the monolithic system; and vi) simulated and experimental results.

II. MOTOR DRIVE SYSTEMS

Both configurations comprise six switches, a dc-link capacitor bank with mid-point connection and two inductions motors (three-phase and single-phase motors). The converter is composed by switches $q_1, \bar{q}_1, q_2, \bar{q}_2, q_3$ and \bar{q}_3 .

A. Three-phase motor model

A typical three-phase machine has been used in this work. Selecting a fixed coordinate reference frame, the mathematical model that describes the dynamic behavior of the three-phase induction motor is given by

$$\mathbf{v}_{sdq} = r_s \mathbf{i}_{sdq} + \frac{d}{dt} \phi_{sdq} \quad (1)$$

$$\mathbf{v}_{rdq} = r_r \mathbf{i}_{rdq} + \frac{d}{dt} \phi_{rdq} - j\omega_r \phi_{rdq} \quad (2)$$

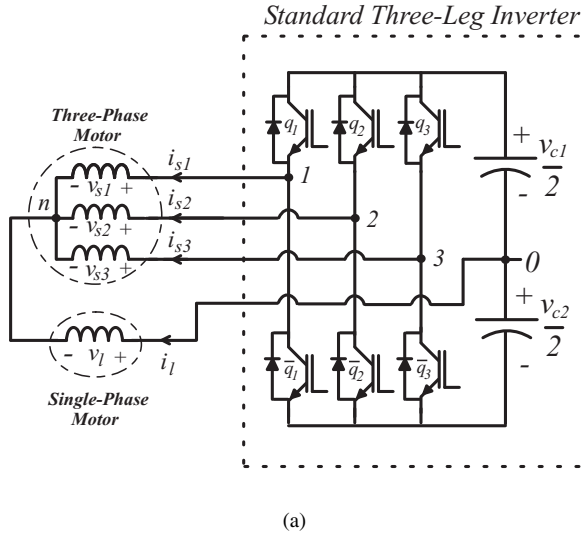
$$\phi_{sdq} = l_s \mathbf{i}_{sdq} + l_{sr} \mathbf{i}_{rdq} \quad (3)$$

$$\phi_{rdq} = l_{sr} \mathbf{i}_{sdq} + l_r \mathbf{i}_{rdq} \quad (4)$$

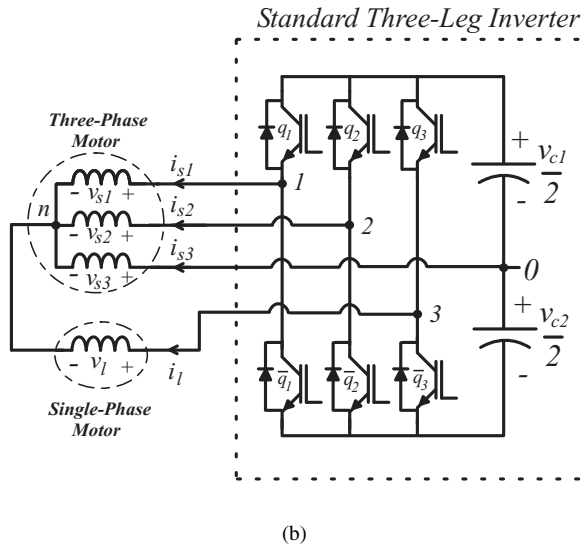
$$v_{so} = r_s i_{so} + l_{ls} \frac{d}{dt} i_{so} \quad (5)$$

$$v_{ro} = r_r i_{ro} + l_{lr} \frac{d}{dt} i_{ro} \quad (6)$$

$$T_e = Pl_{sr}(i_{sq} i_{rd} - i_{sd} i_{rq}) \quad (7)$$



(a)



(b)

Fig. 1. Monolithic systems - standard inverter supplying independently two motors in a series connected scheme: (a) Configuration A and (b) Configuration B.

where $\mathbf{v}_{sdq} = v_{sd} + jv_{sq}$, $\mathbf{i}_{sdq} = i_{sd} + ji_{sq}$, and $\phi_{sdq} = \phi_{sd} + j\phi_{sq}$ are the voltage, current and flux dq vectors of the stator, respectively; v_{so} and i_{so} are the homopolar voltage and current of the stator, respectively (the equivalent rotor variables are obtained by replacing the subscript s by r); T_e is the electromagnetic torque; ω_r is the angular frequency of the rotor; r_s and r_r are the stator and rotor resistances; l_s , l_l , l_r and l_{lr} are the self and leakage inductance of the stator and rotor, respectively; l_{sr} is the mutual inductance and P is the number of pair of poles of the machine.

The dqo stator variables of the previous model can be determined from the 123 variables by using the transformation given by

$$\mathbf{w}_{s123} = \mathbf{A}_s \mathbf{w}_{sdqo} \quad (8)$$

with $\mathbf{w}_{s123} = [w_{s1} \ w_{s2} \ w_{s3}]^T$, $\mathbf{w}_{sdqo} = [w_{sd} \ w_{sq} \ w_{so}]^T$ and

$$\mathbf{A}_s = \sqrt{\frac{2}{3}} \begin{bmatrix} 1 & 0 & \frac{\sqrt{2}}{2} \\ -\frac{1}{2} & \frac{\sqrt{3}}{2} & \frac{\sqrt{2}}{2} \\ -\frac{1}{2} & -\frac{\sqrt{3}}{2} & \frac{\sqrt{2}}{2} \end{bmatrix}.$$

Vectors \mathbf{w}_{s123} and \mathbf{w}_{sdqo} can be voltage or current or flux vectors and $\mathbf{A}_s^{-1} = \mathbf{A}_s^T$.

B. Single-phase motor model

A permanent-capacitor single-phase motor has a capacitor series connected with the auxiliary winding in order to generate the rotating magnetic field. Choice of the capacitor value is made to achieve minimum electromagnetic torque oscillation at rated speed. Despite of be designed to operate under constant frequency it can be shown that there exist a frequency range in which it is possible to vary its speed [11].

III. CONFIGURATION A

A. Model

The first configuration proposed in this work is shown in Fig 1(a). In this topology the single-phase machine is connected to dc-link midpoint. The machine voltages are given by

$$v_{s1} = v_{10} + v_l \quad (9)$$

$$v_{s2} = v_{20} + v_l \quad (10)$$

$$v_{s3} = v_{30} + v_l \quad (11)$$

$$v_l = \frac{1}{3} (\sqrt{3}v_{so} - v_{10} - v_{20} - v_{30}). \quad (12)$$

From (9)-(11) and (8), the dqo voltages of the three-phase machine are obtained as follows

$$v_{sd} = \sqrt{\frac{2}{3}} \left(v_{10} - \frac{1}{2}v_{20} - \frac{1}{2}v_{30} \right) \quad (13)$$

$$v_{sq} = \frac{1}{\sqrt{2}} (v_{20} - v_{30}) \quad (14)$$

$$v_{so} = \frac{1}{\sqrt{3}} (v_{10} + v_{20} + v_{30} + 3v_l). \quad (15)$$

Assuming that i_{si} ($i = 1$ to 3) are phase currents of the three-phase machine, i_{sdqi} ($i = 1$ to 3) are parts of the phase currents only associated to dq currents [given by (8) with $i_{so} = 0$, i.e., $i_{sdq1} = \sqrt{2/3}i_{sd}$, $i_{sdq2} = -\sqrt{1/6}i_{sd} + \sqrt{1/2}i_{sq}$ and $i_{sdq3} = -\sqrt{1/6}i_{sd} - \sqrt{1/2}i_{sq}$] and i_{so} are the o reference current (associated to the single-phase current i_l), the following relation can be defined

$$i_{s1} = i_{sdq1} + i_{so} \quad (16)$$

$$i_{s2} = i_{sdq2} + i_{so} \quad (17)$$

$$i_{s3} = i_{sdq3} + i_{so}. \quad (18)$$

Since $i_{so} = \frac{1}{\sqrt{3}}(i_{s1} + i_{s2} + i_{s3})$ and $i_l = -i_{s1} - i_{s2} - i_{s3}$, the current i_{so} is given by

$$i_{so} = -\frac{i_l}{\sqrt{3}}. \quad (19)$$

In (13)-(15) only variable o depend on v_l . Introducing new voltage variable o' (only depending on pole voltages), that is,

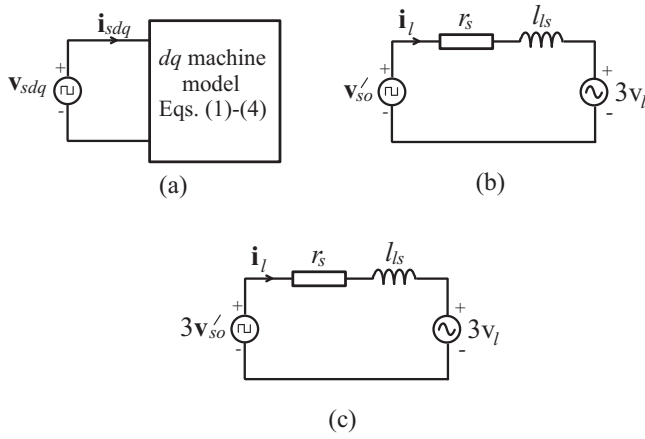


Fig. 2. Equivalent circuits. Configuration A (a) and (b). Configuration B (a) and (c).

$v'_{so} = \sum_{j=1}^3 v_{j0}$, and considering (15), the o model given by (5) become

$$v'_{so} = -r_s i_l - l_{ls} \frac{d}{dt} i_l - 3v_l. \quad (20)$$

Considering (1)-(4) and (20), the model diagram for the dq and o variables can be defined as depicted in Fig. 2(a) and Fig. 2(b), respectively. Note that, only variable o depend on v_l (single-phase machine voltage), the dq model being decoupled from the o model.

B. PWM Control

The pulse-width modulation can be determined directly from system voltages referred to the mid-point of the dc-link (pole voltages), which has been defined from the desired reference machines phase voltages. The reference pole voltages is expressed by

$$v_{10}^* = v_{s1}^* - v_l^* \quad (21)$$

$$v_{20}^* = v_{s2}^* - v_l^* \quad (22)$$

$$v_{30}^* = v_{s3}^* - v_l^*. \quad (23)$$

Once the pole voltage v_{10}^* to v_{30}^* have been determine, the pulse-widths (τ_1 , τ_2 and τ_3) are calculated by using programmable timers or by comparing the modulation reference signal v_{10}^* to v_{30}^* by a high frequency triangular carrier signal.

IV. CONFIGURATION B

A. Model

The second configuration proposed in this work is shown in Fig 1(b). In this topology the three-phase machine is connected to dc-link midpoint. The machine voltages are given by

$$v_{s1} = v_{10} - v_{30} + v_l \quad (24)$$

$$v_{s2} = v_{20} - v_{30} + v_l \quad (25)$$

$$v_{s3} = -v_{30} + v_l \quad (26)$$

$$v_l = -\frac{1}{3}v_{10} - \frac{1}{3}v_{20} + v_{30} + \frac{1}{\sqrt{3}}v_{so}. \quad (27)$$

From (24)-(26) and (8), the dqo voltages of the three-phase machine are obtained as follows

$$v_{sd} = \sqrt{\frac{2}{3}} \left(v_{10} - \frac{1}{2}v_{20} \right) \quad (28)$$

$$v_{sq} = \frac{1}{\sqrt{2}}v_{20} \quad (29)$$

$$v_{so} = \sqrt{3} \left(v_l + \frac{1}{3}v_{10} + \frac{1}{3}v_{20} - v_{30} \right). \quad (30)$$

As observed in Configuration A, only variable o depend on v_l . Introducing new voltage variable o' (only depending on pole voltages), that is, $v'_{so} = \frac{1}{3}v_{10} + \frac{1}{3}v_{20} - v_{30}$, and considering (30), the o model given by (5) become

$$3v'_{so} = -r_s i_l - l_{ls} \frac{d}{dt} i_l - 3v_l. \quad (31)$$

Considering (1)-(4) and (31), the model diagram for the dq and o variables can be defined as depicted in Fig. 2(a) and Fig. 2(c), respectively. Only variable o depend on v_l (single-phase machine voltage), the dq model being decoupled from the o model.

Considering (16)-(18) are still valid for Configuration B.

B. PWM Control

Given the reference voltages v_l^* , v_{s1}^* , v_{s2}^* and v_{s3}^* , then the reference pole voltages can be expressed as

$$v_{10}^* = v_{s1}^* - v_{s3}^* \quad (32)$$

$$v_{20}^* = v_{s2}^* - v_{s3}^* \quad (33)$$

$$v_{30}^* = v_l^* - v_{s3}^*. \quad (34)$$

The pulse-widths (τ_1 , τ_2 and τ_3) are calculated by using programmable timers or by comparing the modulation reference signal v_{10}^* to v_{30}^* by a high frequency triangular carrier signal.

V. CONTROL STRATEGY

The control block diagram of the systems are shown in Fig. 3. In this figure IM 1 represents the three-phase machine, while IM 2 represents the single-phase machine. The dq currents of the three-phase machine are controlled directly by the dq voltages (v_{sdq}^*) by using the controller R_{dq} ; and v_l is controlled with the Volts/Hertz strategy. Block R_{dq} implements the dq currents control. When the torque control is accomplished by control of dq voltages, the diagrams in Fig. 3 can be directly adapted. In this case, the torque controller outputs are the voltages v_{sdq}^* (the controller R_{dq} is eliminated).

VI. CURRENT CONTROLLER

When the current is sinusoidal, a standard PI stationary controller does not guarantee zero sinusoidal steady-state error. Instead, the utilization of a double sequence synchronous controller for single-phase or three-phase systems, as discussed

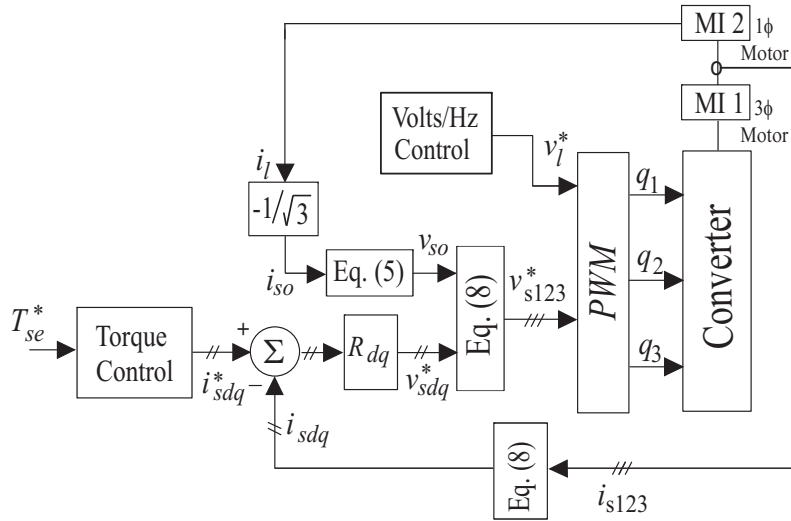


Fig. 3. Control block diagram of the monolithic systems.

in [12], overcomes such difficulty. The simplified controller and has the following continuous-time control law

$$\frac{dx_a}{dt} = x_b + 2k_i \xi_{sm} \quad (35)$$

$$\frac{dx_b}{dt} = -\omega_e^2 x_a \quad (36)$$

$$v_{sm}^* = x_a + k_p \xi_{sm}. \quad (37)$$

In these equations, $\xi_{sm} = i_{sm}^* - i_{sm}$ is the current error ($m = d$ or $m = q$) for the d or q current, respectively; x_a and x_b are state-variables of the controller; v_{sm}^* is the reference voltages; ω_e is the current reference frequency ($\omega_e = \omega_s$, i.e., stator frequency, for dq controllers or $\omega_e = \omega_g$, i.e., grid frequency, for the o controller); and k_p , and k_i are the gains of the controller. This controller gives zero error in the frequency ω_e .

The discrete-time version of controller is given by

$$x_a(k) = \cos(\omega_e h) x_a(k-1) \quad (38)$$

$$+ \frac{1}{\omega_e} \sin(\omega_e h) x_b(k-1) \quad (39)$$

$$+ 2k_i \frac{1}{\omega_e} \sin(\omega_e h) \xi_{sm}(k-1) \quad (40)$$

$$x_b(k) = -\omega_e \sin(\omega_e h) x_a(k-1) \quad (41)$$

$$+ \cos(\omega_e h) x_b(k-1) \quad (42)$$

$$+ 2k_i [\cos(\omega_e h) - 1] \xi_{sm}(k-1) \quad (43)$$

$$v_{sm}^*(k) = x_a(k) + k_p \xi_{sm}(k) \quad (44)$$

where h is the sampling period.

VII. VOLTAGE ANALYSIS

Given the model for the proposed configurations, the following equations can be written to compute the minimum required value of the dc-link voltage for Configuration A and Configuration B, respectively:

$$v_c^* = |v_{sj} - v_{sk}| \quad j, k = 1, 2, 3 \text{ and } j \neq k \quad (45)$$

$$v_c^* = 2|v_l - v_{sj}| \quad j = 1, 2, 3 \quad (46)$$

$$v_c^* = 2|v_l - v_{s3}| \quad (47)$$

$$v_c^* = 2|v_{sj} - v_{s3}| \quad j = 1, 2. \quad (48)$$

The voltage limits have been determined by considering that all voltages are purely sinusoidal. Fig. 4 shows $v_c = f(V_s)$ with $V_l = V_n$, where V_s , V_l and V_n is the phase voltage of three-phase motor, voltage of single-phase motor and rated voltage, respectively. It can be noted that in terms of the dc-link voltage, for $V_s \leq 1.35V_l$ Configuration A requires the same voltage as required for Configuration B, while for $V_s > 1.35V_l$ Configuration A requires a voltage smaller than that of Configurations B.

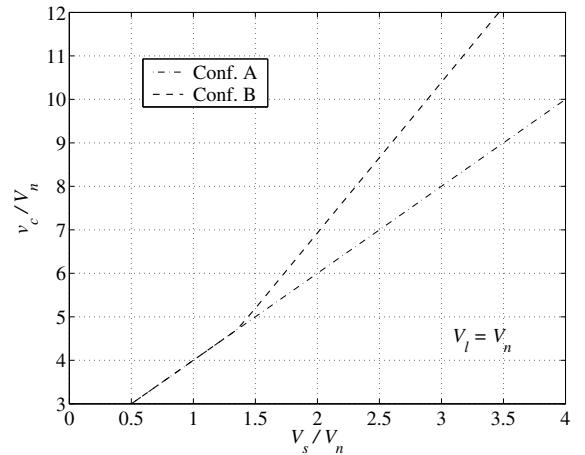


Fig. 4. Dc-link voltage for Configuration A and B with fixed V_l (voltage of single-phase motor) and variable V_s (voltage of three-phase motor).

VIII. CAPACITOR CURRENT ANALYSIS

The capacitor currents are important issues for the proposed configurations due to the dc-link mid-point connection. Neglecting the harmonics related to switching frequency, these

TABLE I
NUMBER OF LEGS REDESIGNED AND THE PERCENTAGE OF THEIR CURRENTS INCREASED.

	Condition I	Condition II	Condition III
Conf. A	3 leg - 8%	3 leg - 3%	3 leg - 2%
Conf. B	2 leg - 8%	2 leg - 3%	2 leg - 2%

currents for Configuration A and for Configuration B can be expressed by:

$$i_{c1} = \frac{i_l}{2} \quad (49)$$

$$i_{c2} = -\frac{i_l}{2} \quad (50)$$

and

$$i_{c1} = \frac{i_{s3}}{2} \quad (51)$$

$$i_{c2} = -\frac{i_{s3}}{2}. \quad (52)$$

Admitting that i_l is smaller than i_s , since the power of the three-phase motor is considered higher than that of power of single-phase motor. Then, in terms of capacitor current the Configuration A is more interesting than Configuration B.

IX. CURRENT OF THE SWITCHES

As observed in (16)-(18) the legs of the proposed configurations need be redesign, due to the presence of the single-phase motor current (extra current - i_l). For Configuration A three legs need be redesigned for larger currents, if compared with conventional three-leg inverter motor drive system. For Configuration B just two legs need be redesigned for larger currents.

In this section three different conditions will be considered: Condition I: Single-phase machine power is 25% of the three-phase machine power ($P_{1\phi} = 0.25P_{3\phi}$); Condition II: Single-phase machine power is 10% of the three-phase machine power ($P_{1\phi} = 0.1P_{3\phi}$); Condition III: Single-phase machine power is 5% of the three-phase machine power ($P_{1\phi} = 0.05P_{3\phi}$); and it will be considered that both machines have the same rated voltage.

Table I shows the number of redesigned legs and the percentage of their currents increased due to presence of the single-phase current, considering Conditions I, II and III. For example, considering Configuration A (see Table I - Condition I), it means that three legs need be designed for larger currents (8% larger), if compared with conventional configuration (three-leg inverter supplying a single three-phase motor).

X. DESIGN OF THE THREE-PHASE MACHINE

The extra current term (i_{so}) in (16)-(18) will be responsible for extra losses in the three-phase machine due to series connection scheme. The aim of this section is to present the ways to make the extra current (i_{so}) less important in terms of system losses and to improve the three-phase machine performance.

In the monolithic systems (see Fig. 1), the induction machines are supplied by a voltage source inverter. Then, with the

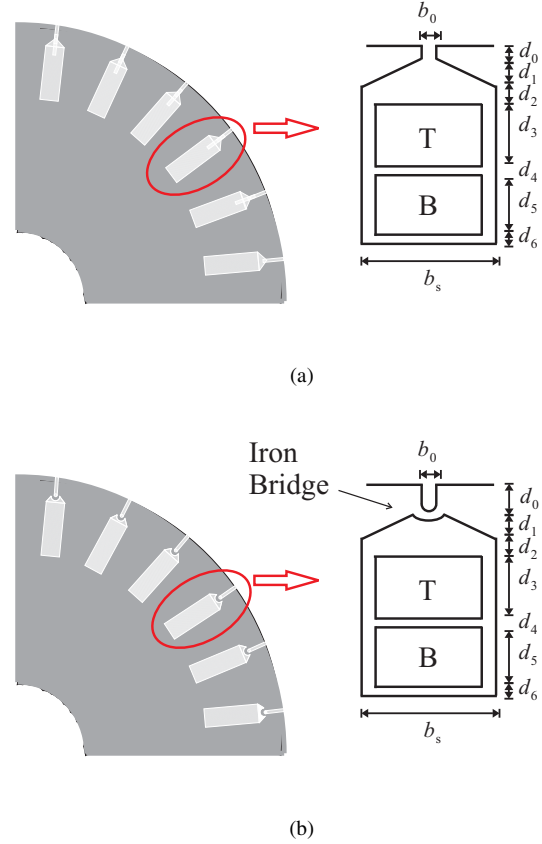


Fig. 5. Rotor slots for induction machines. Conventional design (top). Design for inverter supply (bottom).

inverter as the power supply, the operational conditions of an induction machine are much different from the conventional supply with fixed voltage and frequency [13], which implies that the design of induction machines should be reconsidered to make them more suitable for the inverter-driven variable speed systems. The new design strategies of an induction machine proposed in [13] can be used in the monolithic systems, which make full use of the benefits from the inverter. In a conventional design for commercial power lines, the basic considerations are: 1) to satisfy the required start-up characteristics; 2) to provide appropriate steady state characteristics, emphasizing efficiency and power factor; and 3) to permit easy and economic manufacturing. Items 1), 2) and 3) are generally assigned with weightings of 50%, 30% and 20%, respectively [13]. The conventional design strategy implies that in a standard induction machine design, the primary concern is the start-up characteristics, which include limiting inrush current, generating as much as possible starting torque, and ensuring a high starting efficiency. To meet the start-up requirements, the design strategy is searching for means to maximize the skin effect and to increase the rotor resistance during starting.

However, in designing an induction machine supplied by a voltage source inverter, the strategies are very different.

Weighting assignments to Items 1) through 3) can be entirely changed because the two benefits are gained from the inverter supply, i.e. a) the start-up characteristics with a fixed frequency can be completely ignored; and b) the most favorable slip frequency can be selected to maximize efficiency. Removing the weighting of Item 1) implies that restrictions imposed by rotor slot shape can also be lifted. The design with inverter driven condition allows the stator and rotor slot numbers, shapes, and size to be optimized exclusively for minimizing the leakage inductance and resistance. The advantages associated with the reduced rotor leakage inductance and resistance, such as increased peak torque, improved efficiency and power factor, can be expected.

Particularly, for the monolithic system, the reduction of rotor leakage inductance and resistance (r_s and l_{ls} – see Fig. 2) implies in reduction of losses of the system, as observed in Fig. 2(b) for Configuration A and in Fig. 2(c) for Configuration B.

Additionally, the reduction harmonic winding losses of the rotor is obtained with the change of rotor geometry. Fig. 5(a) shows the induction machine rotor slots conventional design, while Fig. 5(b) special design for the monolithic system. In this case, has been observed a iron bridge at the top of the slot. The thickness of the bridge at the top of the slot is one of the design parameters which determines the magnitude of the leakage flux in the lower part of the slot opening.

XI. EXPERIMENTAL RESULTS

The topologies presented in Fig. 1 have been implemented in the laboratory. In the experimental tests the switching frequency was $10kHz$ and the capacitance of the dc-link capacitor was $2200\mu F$. The set-up used in the experimental tests is based on a microcomputer (PC-Pentium) equipped with appropriate plug-in boards and sensors. A three-phase induction machine (squirrel cage) and a start-capacitor single-phase induction machine was used in this work. Table II shows the ratings of the machines.

Fig. 6 shows the three-phase currents (i_{s1} and i_{s2}) operating at $10Hz$. In spite of the three-phase machine currents present

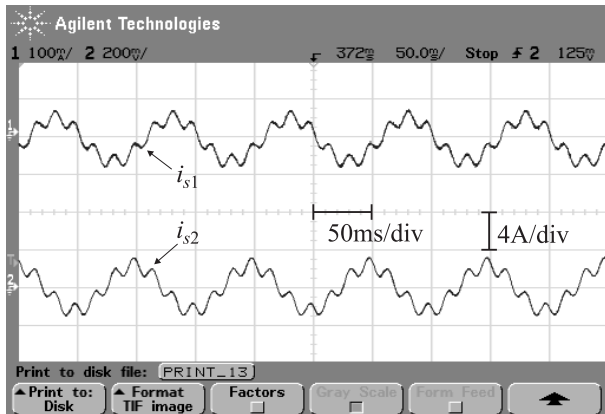


Fig. 6. Experimental results of Configuration A: three-phase currents (i_{s1} , i_{s2}) operating at $10Hz$.

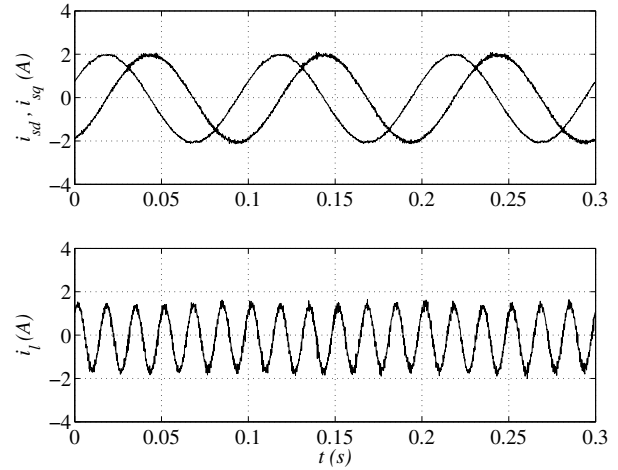


Fig. 7. Experimental results of Configuration B: (a) dq currents of the three-phase machine ($10Hz$) and (b) single-phase machine current ($60Hz$).

TABLE II
RATINGS OF THE MACHINES.

	Three-phase Motor	Single-phase Motor
Power	1HP	1/2HP
Voltage	380V	110V
Current	1.75A	6.5A
$\cos(\phi)$	0.82	0.87
Capacitor	–	$40\mu F - 250V$
speed	1720 rpm	1610 rpm

distortions, as expected, its dq currents are perfectly balanced, as shown in Fig. 7.

Similar results has been obtained with Configuration B, and in the same way the three-phase machine currents present distortions due to the presence of the single-phase current, but dq current are balanced.

As expected the feasibility of the independent control for both machines was demonstrated.

XII. CONCLUSION

This paper has presented two reduced switch count ac drive systems, in which a standard three leg inverter has been used to supply two machines independently. All the proposed topologies employs a single standard three-leg inverter.

Configuration A is the best choice when the capacitor current and capacitor voltage is a critical factor, while Configuration B is more indicated when the redesign of the legs is the critical factor.

Their operating principles were presented and it has been shown that their overall performance are adequate. The experimental results have demonstrated the feasibility of the proposed topologies.

ACKNOWLEDGMENT

The authors would like to thank the financial support provided by the Conselho Nacional de Desenvolvimento Científico e Tecnológico (CNPq) and the Coordenação de Aperfeiçoamento de Pessoal de Nível Superior (CAPES) of Brazil.

REFERENCES

- [1] G. Su and J. Hsu. A five-leg inverter for driving a traction motor and a compressor motor. In *Proc. IEEE APEC*, pages 117–123, 2004.
- [2] C. Klumpner and F. Blaabjerg. Modulation method for a multiple drive system based on a two-stage direct power conversion topology with reduced input current ripple. *IEEE Trans. Power Electron.*, 20(4):922–929, July 2005.
- [3] F. Blaabjerg, D.O. Neacsu, and J.K. Pedersen. Adaptive svm to compensate dc-link voltage ripple for four switch three-phase voltage-source inverters. *IEEE Trans. Power Electron.*, 14(4):743–752, July 1999.
- [4] P. Enjeti and A. Rahman. A new single phase to three phase converter with active input current shaping for low cost ac motor drives. *IEEE Trans. Ind. Applicat.*, 29(2):806–813, July/Aug. 1993.
- [5] H. W. Van der Broeck and J. D. Van Wyk. A comparative investigation of three-phase induction machine drive with a component minimized voltage-fed inverter under different control options. *IEEE Trans. Ind. Applicat.*, 20(2):309–320, March/April 1984.
- [6] S. Kwak and H. A. Toliyat. Design and performance comparisons of two multidrive systems with unity power factor. *IEEE Trans. Power Delivery*, 20(1):417–426, Jan. 2005.
- [7] A. Bouscayrol, B. Francois, P. Delarue, and J. Niiranen. Control implementation of a five-leg ac/ac converter to supply a three-phase induction machine. *IEEE Trans. Power Electron.*, 20(1):107–115, Jan 2003.
- [8] C. B. Jacobina, E. C. dos Santos Jr, M. B. R. Correa, and E. R. C. da Silva. Ac motor drives with a reduced number of switches and boost inductors. *IEEE Trans. Ind. Applicat.*, 43(1):30–39, Jan./Feb. 2007.
- [9] M. Jones, S. N. Vukosavic, E. Levi, and A. Iqbal. A six-phase series-connected two-motor drive with decoupled dynamic control. *IEEE Trans. Ind. Applicat.*, 41(4):1056–1066, July/Aug. 2005.
- [10] J. Itoh and K. Fujita. Novel unity power factor circuits using zero-vector control for single-phase input systems. *IEEE Trans. Power Electron.*, 15(1):36–43, January 2000.
- [11] E. R. Collins Jr., H. B. Puttgen, and W. E. Sayle II. Single-phase induction motor adjustable speed drive: direct phase angle control of the auxiliary winding supply. In *Conf. Rec. IEEE-IAS Annu. Meeting*, pages 246–252, 1988.
- [12] C. B. Jacobina, M. B. R. Correa, T. M. Oliveira, A. M. N. Lima, and E. R. C. da Silva. Current control of unbalanced electrical systems. In *Conf. Rec. IEEE-IAS Annu. Meeting*, pages 1011–1017, 1999.
- [13] Z. M. Zhao, S. Meng, C. C. Chan, and E. W. C. Lo. A novel induction machine design suitable for inverter-driven variable speed systems. *IEEE Trans. Energy Conv.*, 15(4):413–420, Dec. 2000.